# Synthesis, Structure, and Magnetic Properties of Mn(salpn)$N_3$, a Helical Polymer, and Fe(salpn)$N_3$, a Ferromagnetically Coupled Dimer (salpn$H_2$ = *N*,*N*′-bis(Salicylidene)-1,3-diaminopropane)

**K. Rajender Reddy,[†] M. V. Rajasekharan,*[,†] and J.-P. Tuchagues*[,‡]**

School of Chemistry, University of Hyderabad, Hyderabad 500046, India, and Laboratoire de Chimie de Coordination du CNRS, UP 8241 liée par conventions à l'Université Paul Sabatier et à l'Institut National Polytechnique, 205 route de Narbonne, 31077 Toulouse Cèdex, France

*Received December 22, 1997*

The preparation, crystal structures, and variable temperature magnetic susceptibility data are presented for two azido-bridged Schiff base complexes of Mn(III) and Fe(III). Mn(salpn)$N_3$ (**1**), where salpn is the dianion of *N*,*N*′-bis(salicylidene)-1,3-diaminopropane, crystallizes in the orthorhombic system, space group $Pna2_1$, with $a$ = 11.947(2) Å, $b$ = 11.818(2) Å, $c$ = 11.227(5) Å, and $Z$ = 4. Fe(salpn)$N_3$ (**2**) crystallizes in the monoclinic system, space group $P2_1/c$, with $a$ = 10.199(7) Å, $b$ = 14.081(6) Å, $c$ = 12.017(3) Å, $\beta$ = 105.19(3)°, and $Z$ = 4. In **1**, salpn coordinates in the equatorial mode, with two azide ions coordinating in axial positions. The azide ions act as "end-to-end" ($\mu$-(1,3)) bridges, leading to an infinite helical chain propagating along the crystallographic *c* axis. In striking contrast, **2** has a dimeric structure in which the Schiff base adopts a cis-octahedral coordination mode. The dimer is held together by two "head-on" ($\mu$-(1,1)) bridging azide ions. The polymeric compound, **1,** is weakly antiferromagnetic ($J = -4.03$ cm$^{-1}$, $H_{ex} = -2J\sum S_iS_{i+1}$), while **2** is weakly ferromagnetic ($J = 0.76$ cm$^{-1}$, $H_{ex} = -2JS_1S_2$).

## Introduction

The pseudohalide ions, $N_3^-$, $NCS^-$, and $NCO^-$ have been well exploited for their ability to bridge paramagnetic moeities into dimers, clusters, and polymers.[1] These ions, especially $N_3^-$, exhibit different bridging modes, viz., $\mu$-(1,3),[2] $\mu$-(1,1),[3] and (rarely) $\mu$-(1,1,1),[4] the latter two modes leading to ferromagnetic interactions. There are very few structurally characterized complexes of Mn(III)[2d] and Fe(III)[3d] with pseudohalide bridges. Mn(acac)$_2$X has a linear chain structure when X is azide or thiocyanate[2d,5a] (acacH = acetylacetone). Mn(salen)X is also believed to have a similar structure based on spectral and magnetic studies,[5b] but no crystallographic data are available for these complexes (salen$H_2$ = 1,2-bis(salicylideneamino)-ethane). While tetradentate Schiff base (SB) ligands similar to salen are the natural choice for making neutral M(III) pseudohalide complexes of the type M(SB)X, to our knowledge, no such complexes of Mn and Fe have been structurally characterized so far. We find that the use of salpn in place of salen leads to the crystallizable complexes Mn(salpn)$N_3$ (**1**) and Fe(salpn)$N_3$ (**2**), which form the subject of this paper. Some complexes of salpn[6] with Mn(III)[7,8] and Fe(III)[9] have been previously reported. Being more flexible than salen, salpn allows both equatorial[7,8] and cis-octahedral[8] modes of ligation. In **1**, salpn adopts the equatorial mode and $N_3^-$ functions as a $\mu$-(1,3) bridging ligand, leading to a polymeric chain. The iron analogue (**2**), on the other hand, is a cis-bridged dimer having two $\mu$-(1,1) $N_3^-$ ions. The polymeric chains in **1** are of the helical type.

## Experimental Section

Salicylaldehyde and 1,3-diaminopropane were of reagent grade. The Schiff base was formed in situ in the presence of the appropriate metal salt.

**Mn(salpn)$N_3$ (1).** In a beaker open to the atmosphere, 229 mg (1.88 mmol) of salicylaldehyde and 71 mg (0.96 mmol) of 1,3-diaminopropane were stirred into 40 mL of ethanol. $Mn(CH_3CO_2)_2\cdot 4H_2O$ in an amount of 245 mg (1.00 mmol) was added, and the stirring was continued for about 0.5 h. To the resulting solution, 130 mg (2.00 mmol) of $NaN_3$ dissolved in a minimum amount of water was added. The solution was allowed to stand for about 3 h to complete the air oxidation of Mn(II). The filtered solution was then kept aside for 2

[†] University of Hyderabad.
[‡] Laboratoire de Chimie de Coordination du CNRS.

(1) Vrieze, K.; van Koten, G. In *Comprehensive Coordination Chemistry*; Wilkinson, G., Gillard, R. D., McCleverty, J. A., Eds; Pergamon Press: Oxford, England, 1987; Vol. 2, p 225 and references therein.
(2) (a) Ribas, J.; Monfort, M.; Ghosh, B. K.; Cortes, R.; Solans, X.; Font-Bardia, M. *Inorg. Chem.* **1996**, *35*, 864. (b) Tuczek, F.; Bensch, W. *Inorg. Chem.* **1995**, *34*, 1482. (c) Escuer, A.; Vicente, R.; Goher, M. A. S.; Mautner, F. A. *Inorg. Chem.* **1995**, *34*, 5707. (d) Stults, B. R.; Marianelli, R. S.; Day, V. W. *Inorg.* Chem. **1975**, *14*, 722.
(3) (a) Ribas, J.; Monfort, M.; Diaz, C.; Bastos, C.; Solans, X. *Inorg. Chem.* **1994**, *33*, 484. (b) Mautner, A. F.; Goher, M. A. S. *Polyhedron* **1996**, *15*, 1133. (c) Cortes, R.; Pizarro, J. L.; Lezama, L.; Arriortua, M. I.; Rojo, T. *Inorg. Chem.* **1994**, *33*, 2697. (d) De Munno, D.; Poerio, T.; Viau, G.; Julve, M.; Lloret, F. *Angew. Chem., Int. Ed. Engl.* **1997**, *36*, 1459.
(4) Wemple, M. W.; Adams, D. M.; Hagen, K. S.; Folting, K.; Hendrickson, D. N.; Christou, G. *J. Chem. Soc., Chem. Commun.* **1995**, 1591.
(5) (a) Gregson, A. K.; Moxon, N. T. *Inorg. Chem.* **1982**, *21*, 586. (b) Kennedy, B. J.; Murray, K. S. *Inorg. Chem.* **1985**, *24*, 1552.
(6) Hariharan, M.; Urbach, F. L. *Inorg. Chem.* **1969**, *8*, 556.
(7) Aurangzeb, N.; Hulme, C. E.; McAuliffe, C. A.; Pritchard, R. G.; Watkinson, M.; Gracia-Deibe, A.; Bermejo, M. R.; Sousa, A. *J. Chem. Soc., Chem. Commun.* **1992**, 1524.
(8) Gohdes, J. W.; Armstrong, W. H. *Inorg. Chem.* **1992**, *31*, 368.
(9) Smékal, Z.; Brezina, F.; Sindelár, Z.; Klicka, R. *Polyhedron* **1996**, *15*, 1971.

10.1021/ic971592y CCC: $15.00 
Published on Web 10/29/1998

**Table 1.** Crystallographic Data

| | **1** | **2** |
|---|---|---|
| formula | $C_{17}H_{16}MnN_5O_2$ | $C_{17}H_{16}FeN_5O_2$ |
| fw | 377.29 | 378.20 |
| *a* | 11.947(2) Å | 10.199(7) Å |
| *b* | 11.818(2) Å | 14.081(6) Å |
| *c* | 11.227(5) Å | 12.017(3) Å |
| $\beta$ | | 105.19(3)° |
| *V* | 1585.2(8) Å$^3$ | 1666(1) Å$^3$ |
| *Z* | 4 | 4 |
| space group | *Pna*2$_1$(no. 33) | *P*2$_1$/*c*(no. 14) |
| *T* | 20 °C | 20 °C |
| $\lambda$ | 0.710 73 Å | 0.710 73 Å |
| $\rho_{calcd}$ | 1.581 g cm$^{-3}$ | 1.508 g cm$^{-3}$ |
| $\mu$ | 8.55 cm$^{-1}$ | 9.27 cm$^{-1}$ |
| $R(F_o^2)^a$ | 0.0260 | 0.0525 |
| $R_w(F_o^2)^b$ | 0.0617 | 0.1156 |

$^a$ $R = \sum||F_o| - |F_c||/\sum|F_o|$. $^b$ $R_w = [\sum w(F_o^2 - F_c^2)^2/\sum(wF_o^4)]^{1/2}$; $w^{-1} = [\sigma^2(F_o^2) + (AP)^2 + BP]$. $P = (F_o^2 + 2F_c^2)/3$, with $A = 0.0386$ and $B = 0.39$ for **1** and $A = 0.642$ and $B = 2.37$ for **2**.

days over which time green crystals deposited. Yield: 280 mg (0.74 mmol, 79%). Anal. Calcd for $MnC_{17}H_{16}N_5O_2$: C, 54.12; H, 4.27; N, 18.56. Found: C, 54.1; H, 4.2; N, 19.1. Important IR absorptions (cm$^{-1}$): 3350 (b), 2033 (s), 1612 (s), 1541(s).

**Fe(salpn)$N_3$ (2).** Amounts of 229 mg (1.88 mmol) of salicylaldehyde and 71 mg (0.96 mmol) of 1,3-diaminopropane were stirred into 40 mL of ethanol. $Fe(NO_3)_3 \cdot 9H_2O$ in the amount of 404 mg (1.00 mmol) was added, and the mixture was stirred to obtain a clear solution. To this, a solution of 130 mg (2.0 mmol) of $NaN_3$ in a minimum amount of water was added, and the solution was filtered after 2 h. The filtrate was kept overnight yielding a microcrystalline precipitate. The precipitate was separated and dried. Yield: 220 mg (0.58 mmol, 62%). It was recrystallized from $CH_3CN$ to obtain dark-brown X-ray quality crystals. Anal. Calcd for $FeC_{17}H_{16}N_5O_2$: C, 53.98; H, 4.26; N, 18.52. Found: C, 54.6; H, 4.4; N, 17.5. Important IR absorptions (cm$^{-1}$): 3250 (b), 2051 (s), 1670 (m), 1616 (s).

**Crystallography.** X-ray data were collected for **1** and **2** on an Enraf-Nonius CAD4 diffractometer at room temperature using graphite monochromated Mo K$\alpha$ radiation. An empirical absorption correction based on a $\psi$-plot[10a] was applied. The structures were solved by a combination of heavy atom and direct methods using SHELXS-86[10b] and refined using SHELXL-93.[10c] Non-hydrogen atoms were refined anisotropically while the hydrogen atoms were treated using the riding model. Crystal data are in Table 1, and selected bond distances and angles are in Table 2.

**Magnetic Measurements.** The magnetic susceptibility was measured for **1** and **2** in the 2−300 K temperature range using a Quantum Design MPMS SQUID susceptometer. The samples were pressed into pellets to avoid orientation effects of the microcrystals. Diamagnetic corrections were applied using Pascal's constants. Fitting of the susceptibility data was initially done using the program SUSCEP[11] based on the equation of Hiller et al.[12] for **1** and the dimer equation[13] for **2**. Final fittings were carried out by exact diagonalization[14] of the spin-Hamiltonian for **2**. In the case of **1**, more meaningful parameters were obtained using the Heisenberg chain equation of Koenig et al.[15]

**Table 2.** Selected Bond Lengths (Å) and Angles (deg)$^a$

Mn(salpn)$N_3$ (**1**) Bond Distances

| | | | |
|---|---|---|---|
| Mn−O(1) | 1.875(2) | Mn−O(2) | 1.881(3) |
| Mn−N(2) | 2.016(3) | Mn−N(1) | 2.056(3) |
| Mn−N(3) | 2.331(4) | Mn−N(5) | 2.348(4) |
| N(3)−N(4) | 1.165(5) | N(4)−N(5) (no. 1) | 1.190(5) |

Mn(salpn)$N_3$ (**1**) Bond Angles

| | | | |
|---|---|---|---|
| O(1)−Mn−O(2) | 85.9(1) | O(1)−Mn−N(2) | 173.6(1) |
| O(2)−Mn−N(2) | 88.7(1) | O(1)−Mn−N(1) | 91.5(1) |
| O(2)−Mn−N(1) | 176.3(1) | N(2)−Mn−N(1) | 94.0(1) |
| O(1)−Mn−N(3) | 94.5(2) | O(2)−Mn−N(3) | 93.9(1) |
| N(2)−Mn−N(3) | 89.4(1) | N(1)−Mn−N(3) | 83.7(1) |
| O(1)−Mn−N(5) | 88.1(2) | O(2)−Mn−N(5) | 102.1(1) |
| N(2)−Mn−N(5) | 89.6(1) | N(1)−Mn−N(5) | 80.5(1) |
| N(3)−Mn−N(5) | 164.0(1) | N(4)−N(3)−Mn | 137.8(3) |
| N(3)−N(4)−N(5) (no. 1) | 178.7(4) | N(4) (no. 2)−N(5)−Mn | 117.3(3) |

Fe(salpn)$N_3$ (**2**) Bond Distances

| | | | |
|---|---|---|---|
| Fe−O(1) | 1.897(4) | Fe−O(2) | 1.917(4) |
| Fe−N(3) | 2.087(4) | Fe−N(1) | 2.131(4) |
| Fe−N(2) | 2.144(5) | Fe−N(3) (no. 1) | 2.150(4) |
| N(3)−N(4) | 1.223(7) | N(4)−N(5) | 1.148(7) |

Fe(salpn)$N_3$(**2**) Bond Angles

| | | | |
|---|---|---|---|
| O(1)−Fe−O(2) | 93.5(2) | O(1)−Fe−N(3) | 97.1(2) |
| O(2)−Fe−N(3) | 92.7(2) | O(1)−Fe−N(1) | 87.0(2) |
| O(2)−Fe−N(1) | 106.1(2) | N(3)−Fe−N(1) | 160.5(2) |
| O(1)−Fe−N(2) | 169.7(2) | O(2)−Fe−N(2) | 86.5(2) |
| N(3)−Fe−N(2) | 93.2(2) | N(1)−Fe−N(2) | 83.2(2) |
| O(1)−Fe−N(3) (no. 1) | 92.6(2) | O(2)−Fe−N(3) (no. 1) | 165.0(2) |
| N(3)−Fe−N(3) (no. 1) | 72.9(2) | N(1)−Fe−N(3) (no. 1) | 87.9(2) |
| N(2)−Fe−N(3) (no. 1) | 90.0(2) | N(4)−N(3)−Fe | 123.2(4) |
| N(4)−N(3)−Fe (no. 1) | 124.6(4) | Fe−N(3)−Fe (no. 1) | 107.1(2) |
| N(5)−N(4)−N(3) | 176.8(6) | | |

$^a$ Symmetry transformations used to generate equivalent atoms. **1**: (no. 1) $-x, -y, z - 1/2$; (no. 2) $-x, -y, z + 1/2$. **2**: (no. 1) $-x, -y, -z$.

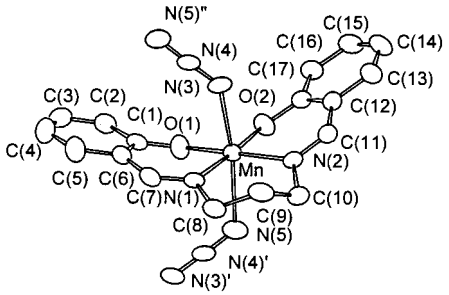


**Figure 1.** ORTEP view of one complex cation and its two bonded azide anions along the 1D chains of $[Mn(salpn)N_3]_n$ in **1**. Hydrogen atoms are omitted for clarity, and the thermal ellipsoids are represented at the 50% probability level (prime = $-x, -y, z + 1/2$; double prime = $-x, -y, z - 1/2$).

## Results and Discussion

**Structure of 1.** The coordination of Mn(III) is to one salpn ligand binding in the equatorial mode and two $N_3^-$ ions in axial positions (Figure 1). Each azide functions as a trans-$\mu$-(1,3) bridge, resulting in a one-dimensional polymer (Figure 2). The chain structure belongs to a modification of the type I azide chain based on a recent classification by Escuer et al.[16] A few polymeric structures, most of them containing acetate bridges, have been previously reported for Mn(III) complexes.[7,17] The unique feature of the present chain is that each monomeric unit is related to its adjacent ones by a 2-fold screw axis, leading to a spiral (or helix) propagating along the crystallographic *c* axis.

(10) (a) North, A. C. T.; Phillips, D. C.; Mathews, F. S. *Acta Crystallogr.* **1968**, *A24*, 351. (b) Sheldrick, G. M. SHELXS-86. *Acta Crystallogr., Sect. A* **1990**, *46*, 467. (c) Sheldrick, G. M. *SHELXL-93*; University of Goettingen: Germany, 1993.
(11) Chandramouli, G. V. R.; Balagopalakrishna, C.; Rajasekharan, M. V.; Manoharan, P. T. *Comput. Chem.* **1996**, *20*, 353. The residual is defined as $R = \sum(\chi_M^o - \chi_M^c)^2/\sum(\chi_M^o)^2$.
(12) Hiller, W.; Straehle, J.; Datz, A.; Hanack, M.; Hatfield, W. E.; der Haar, L. W.; Guetlich, P. *J. Am. Chem. Soc.* **1984**, *106*, 329.
(13) O'Connor, C. J. *Prog. Inorg. Chem.* **1982**, *29*, 203.
(14) (a) Mabad, B.; Cassoux, P.; Tuchagues, J. P.; Hendrickson, D. N. *Inorg. Chem.* **1986**, *25*, 1420. (b) Laskowski, E. J.; Hendrickson, D. N. *Inorg. Chem.* **1978**, *17*, 457.
(15) Koenig, E.; Desai, V. P.; Kanallakopulos, B.; Klenze, R. *Chem. Phys.* **1980**, *54*, 109.
(16) Escuer, A.; Vicente, R.; Fallah, M. S. E.; Ribas, J.; Solans, X. *J. Chem. Soc., Dalton Trans.* **1993**, 2973.

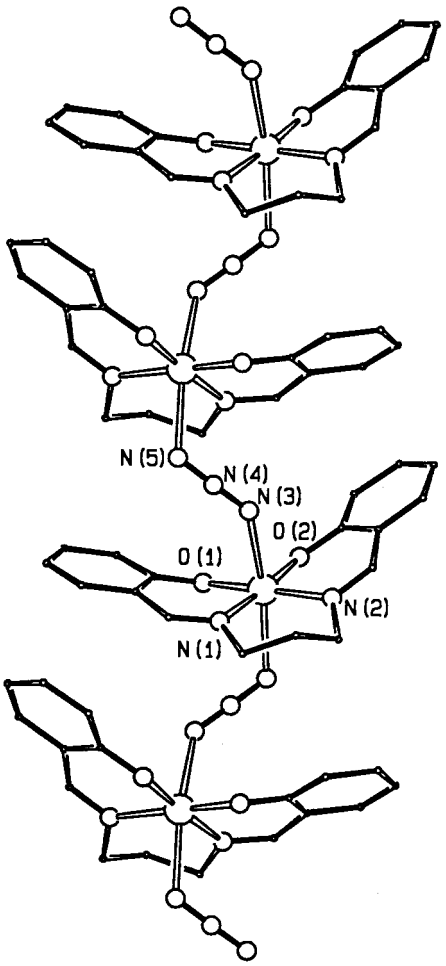


**Figure 2.** Perspective view of helical polymeric chains in **1**.

The equatorial atoms Mn, N(1), N(2), O(1), and O(2) are nearly coplanar (rms deviation = 0.05 Å). The two halves of the SB ligand, excluding the methylene groups, are also individualy planar (rms deviation = 0.04 Å), with the Mn deviating by 0.51 and 0.57 Å from these planes. The two halves are inclined toward each other by 44.0(1)°. The two Mn−O distances are equal and comparable to those in the monomeric compound, $[Mn(salpn)(C_2H_5OH)_2]ClO_4$.[8] However, at variance with the monomeric compound, the two Mn−N distances in **1** are significantly different (2.016(3) and 2.056(3) Å). We attribute this to the steric requirement of the spiral formation. As expected for the Jahn−Teller ion, the axial Mn−N(3) and Mn−N(5) distances (2.331(4) and 2.348(4) Å, respectively) are considerably longer.

**Structure of 2.** The salpn ligand adopts a cis-octahedral tetradentate coordination mode. The azide ion acts as a $\mu$-(1,1) bridge. The dimer depicted in Figure 3 results from the presence of two such bridges cis to each other. The two halves of the dimer are related by a crystallographic inversion center. The structure is comparable to that of the Mn(IV) di-$\mu$-oxo-bridged dimer, $Mn_2O_2(salpn)_2$.[8] The equatorial atoms Fe, N(1), O(2), N(3), and N(3)′ are very nearly coplanar (rms = deviation 0.03 Å). The remaining atoms of the azide ion, N(4) and N(5), deviate by 0.41 and 0.76 Å, respectively, from this plane. The bond distances are close to each other (compared to those of **1**) and do not show any significant difference between equatorial and axial lengths.

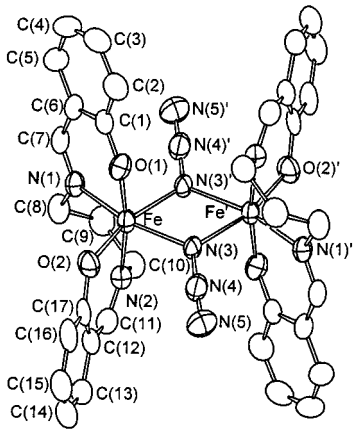


**Figure 3.** ORTEP view of the $[Fe(salpn)N_3]_2$ dinuclear complex molecule in **2**. Hydrogen atoms are omitted for clarity, and the thermal ellipsoids are represented at the 50% probability level (prime = $-x$, $-y$, $-z$).

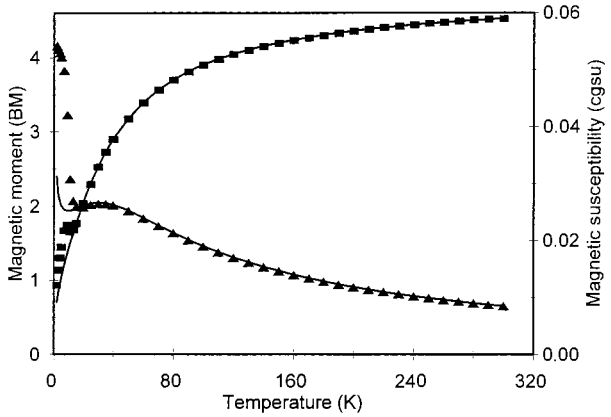


**Figure 4.** Variable-temperature magnetic susceptibility data for **1**. Experimental points are represented by triangles (molar susceptibility) and rectangles (effective magnetic moment). The solid lines result from a least-squares fit of the data to the theoretical values calculated as mentioned in the text.

The azide ion in **2** is less symmetrical than that in **1** (N−N = 1.165(5) and 1.190(5) Å in **1** and 1.148(7) and 1.223(7) Å in **2**). Both compounds show a single sharp absorption corresponding to the N−N stretching vibration (2033 $cm^{-1}$ in **1**; 2050 $cm^{-1}$ in **2**). Such differences arising from the different coordination modes of $N_3^-$ have already been observed in azide complexes.[3c]

**Magnetic Properties.** The thermal variation of the effective magnetic moment shows that **1** (Figure 4) is weakly antiferromagnetic, while **2** (Figure 5) is weakly ferromagnetic. On the basis of Escuer's classification,[16] the linear chain in **1** requires one $g$ and one $J$ for fitting the susceptibility data. Assuming a Heisenberg chain of $S = 2$ ions, the data above 15 K could be fitted to the expression of Hiller et al.,[12] provided interchain coupling is taken into account using the molecular field approximation.[13] The best fit (not shown) gave $J = -3.12$ $cm^{-1}$, $zJ' = -2.07$ $cm^{-1}$, $g = 2.062$, and a residual $(R)^{11} = 3.5 \times 10^{-5}$. In the absence of interchain contacts in the crystal, the comparable magnitudes of interchain ($zJ'$) and intrachain ($J$) coupling parameters cast some doubts upon the validity of the above model. It has been pointed out before[5] that the value of $zJ'$ is influenced by other interactions besides interchain

(17) (a) Davies, J. E.; Gatehouse, B. M.; Murray, K. S. *J. Chem. Soc., Dalton Trans.* **1973**, 2523. (b) Akhtar, F.; Drew, M. G. B. *Acta Crystallogr., Sect. B* **1982**, *38*, 612. (c) Bonadies, J. A.; Kirk, M. L.; Lah, M. S.; Kessissoglou, D. P.; Hatfield, W. E.; Pecoraro, V. L. *Inorg. Chem.* **1989**, *28*, 2037. (d) For a salicylate bridged structure, see: Kirk, M. L.; Lah, M. S.; Raptopoulou, C.; Kessissoglou, D. P.; Hatfield, W. E.; Pecoraro, V. L. *Inorg. Chem.* **1991**, *30*, 3900.

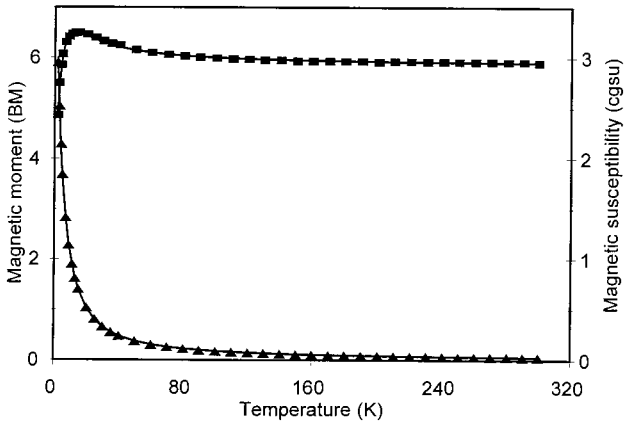


**Figure 5.** Variable-temperature magnetic susceptibility data for **2**. Experimental points are represented by triangles (molar susceptibility) and rectangles (effective magnetic moment). The solid lines result from a least-squares fit of the data to the theoretical values calculated as mentioned in the text.

coupling. A more physically meaningful fit was obtained by using the equation of Koenig et al.,[15] wherein the interchain interaction is accounted for by an empirical correction term, $\theta$. An excellent fit (Figure 4) of the data above 20 K is obtained with $J = -4.03$ cm$^{-1}$, $\theta = 0.022$ K, $g = 1.985$, paramagnetic impurity = 0.6%, and $R = 5 \times 10^{-5}$. The models are unable to reproduce the sharp increase in susceptibilty observed below 15 K. The effect of a paramagnetic impurity is felt only at temperatures lower than 5 K. Furthermore, the expected negative zero-field splitting ($D$) cannot explain the observed magnetic susceptibility variation below 15 K. On the other hand, this sharp increase is reminiscent of a phase transition triggered by a three-dimensional magnetic ordering. As explained by Gregson et al.[5a] and Kennedy and Murray,[5b] the driving force for such a transition is the increasing population of the lower energy magnetic levels of the tetragonally elongated $Mn^{3+}$ ion in this complex. The three-dimensional ordering also requires some intermolecular interaction between chains. The small interaction implied by the $\theta$ value of 0.022 K appears to be sufficient to cause this ordering below ~15 K.

The data for **2** above 20 K could be fitted to the dimer equation for two equivalent $S = 5/2$ ions.[13] The best fit gave $J = 1.054$ cm$^{-1}$, $zJ' = -0.099$ cm$^{-1}$, $g = 1.964$, and $R = 5.1 \times 10^{-6}$. Exact diagonalization of the spin Hamiltonian including axial Zeeman and zero-field terms and isotropic exchange allows a fitting of the full 2−300 K temperature range. However, the fitting is not unique. Two sets of parameters are obtained with acceptable residuals:[18] (1) $J = 1.3$ cm$^{-1}$, $D = 9.3$ cm$^{-1}$, $g_x = g_y = 1.784$, $g_z = 2.305$, $R = 3 \times 10^{-4}$; (2) $J = 0.76$ cm$^{-1}$, $D = -1.3$ cm$^{-1}$, $g_x = g_y = 2.007$, $g_z = 1.917$, $R = 4 \times 10^{-3}$. Solution 1 could be rejected on the following basis. The **g** tensor anisotropy is unusually large for a $^6$S state ion in a distorted octahedral coordination. It appears that the $g$ parameters have absorbed the errors arising from the assumption of an axial zero-field tensor. Since the single ion geometry is of the "C2-distorted octahedron" type, the assumption of an axial $D$ will not be a good approximation when $|D|$ is large. The second solution is most likely closer to the physical situation. The X-band EPR spectrum of the powder sample at 120 K consists of a single broad (1100 G, peak-to-peak) band centered around $g = 2.1$, which is inconsistent with large **g** anisotropy.

(18) The residual here is significantly higher than that for **1**, probably due to correlations within the larger parameter set.

The weak antiferromagnetic coupling in **1** is consistent with earlier observations on Mn(III) linear chain complexes.[5,17a] Due to Jahn−Teller elongation, the only magnetic orbital that can make a signicant contribution to the coupling is the one derived from the Mn(III) $d_{z^2}$ orbital. The axial ligands will provide a (mainly) $\sigma$-type superexchange pathway. However, due to the weakened axial overlap, this can only produce a weak interaction. In this context, it may be noted that azide-bridged linear chains of Ni(II)[19] have $J$ values in the range −24 to −70 cm$^{-1}$.

The ferromagnetic coupling in **2** is consistent with the widespread observation of ferromagnetic interactions in Cu(II), Ni(II), and Mn(II) dimers having one or more $\mu$-(1,1) azide ligands.[3] The weak coupling in **2** is almost certainly due to the near cancellation of ferro- and antiferromagnetic exchange couplings between the two Fe(III) centers. There are two reports of di-$\mu$-(1,1)-azide-bridged complexes of $d^5$ ions, viz., $[Mn(terpy)(N_3)_2]_2$[3c] and $[Fe_2(N_3)_{10}]^{4-}$ (terpy = 2,2′,2″-terpyridine).[3d] Both are weakly ferromagnetic with $J$ values of 1.2 cm$^{-1}$($Mn^{2+}$) and 2.40 cm$^{-1}$($Fe^{3+}$). The difference, despite similar bridge geometry for the two species (Mn−N−Mn = 104.6(1)°; Mn−N = 2.182(3), 2.272(2) Å; Fe−N−Fe = 106.0(2); Fe−N = 2.164(5), 2.195(5) Å), has been attributed to the more favorable energy match between the d orbitals of $Fe^{3+}$ and the HOMO of $N_3^-$, which enhances the ferromagnetic interaction via the spin-polarization mechanism.[20] The present $Fe^{3+}$ complex, which has a slightly different bridge geometry (Fe−N−Fe = 107.1(2)°; Fe−N = 2.087(4), 2.150(4) Å), has a smaller $J$ value (0.76 cm$^{-1}$). The presence of significant zero-field splitting ($D = -1.3$ cm$^{-1}$) also points to the differing magnetic interactions in this compound. No simple correlations based on this variation can be offered except to state that, while the ferromagnetic interaction may be similar in the two Fe(III) compounds, the antiferromagnetic contribution could be significantly different. The latter contribution involves five magnetic orbitals on each center and will be greatly influenced by the coordination polyhedra of the individual ions. In this context, it may be mentioned that dinuclear Fe(III) complexes having the $[Fe_2(O)(OAc)_2]^{2+}$ core are always strongly antiferromagnetically coupled ($J \approx -200$ cm$^{-1}$). This has been explained by the strong overlap of half occupied $d_{z^2}$ and $d_{xz}$ orbitals on the two Fe(III) ions.[21] Such a "crossed pathway" may not be operative in **2** due to the very different ligand-field symmetry. The situation in **2** is somewhat analogous to that of a weakly antiferromagnetic ($J = -2.8$ cm$^{-1}$) dinuclear Fe(III) complex having two alkoxy bridges.[22]

## Conclusion

The main electronic factor distinguishing Mn(III) from Fe(III) is the Jahn−Teller effect, which usually manifests as a tetragonal elongation. This factor appears to control the stereochemistry of the coordination of the flexible SB ligand. The Mn(III) azide-bridged linear chain with long axial bonds has only one dominant exchange pathway, which results in a weak antiferromagnetic interaction due to the small axial overlap. The interaction is, however, stronger than that found earlier for carboxylate bridged Mn(III) polymers,[5b,17] which have $J$ values less than 2.0 cm$^{-1}$.

(19) Escuer, A.; Vicente, R.; Ribas, J.; Fallah M. S. E.; Solans, X.; Font-Bardia, M. *Inorg. Chem.* **1993**, *32*, 3727.
(20) Charlot, M. F.; Kahn, O.; Chaillet, M.; Larrieu, C. *J. Am. Chem. Soc.* **1986**, *108*, 2574.
(21) Hotzelmann, R.; Wiegardt, K.; Floerke, U.; Haupt, H.-J.; Weatherburn, D. C.; Bonvoisin, J.; Blondin, G.; Girerd, J.-J. *J. Am. Chem. Soc.* **1992**, *114*, 1681.
(22) Mikuriya, M.; Yamato, Y.; Tokii, T. *Chem. Lett.* **1992**, 1571.

Magnetostructural correlations for $\mu$-(1,1)-$N_3$-bridged dimers have been previously made for Cu(II) complexes,[20] based on the spin-polarization model. Spin-polarization was also suggested to explain the ferromagnetic coupling in a tetranuclear Ni(II) complex[23] as well as dinuclear Fe(III)[3d] and Mn(II)[3c] complexes. The present Fe(III) complex is also weakly ferromagnetic, like the other two complexes of $d^5$ ions. More such systems need to be characterized before correlations can be attempted. It is noteworthy that despite several orbital pathways, some of which are bound to be antiferromagnetic, the net interaction is ferromagnetic as in other $\mu$-(1,1)-azido complexes.

**Acknowledgment.** K.R.R. thanks CSIR, India for the award of a research associateship.

**Note Added in Proof.** A communication describing the compound **1** obtained through a slightly different route has been published recently.[24]

**Supporting Information Available:** An X-ray crystallographic file, in CIF format, for complexes **1** and **2** is available on the Internet only. Access information is given on any current masthead page.

IC971592Y

(23) Ribas, J.; Monfort, M.; Costa, R.; Solans, X. *Inorg. Chem.* **1993**, *32*, 695.

(24) Li, H.; Zhong, Z. J.; Duan, C.-Y; You, X.-Z.; Mak, T. C. W.; Wu, B. *Inorg. Chim. Acta* **1998**, *271*, 99.